Panel Method Based Guidance for Fixed Wing Micro Aerial Vehicles

Zeynep Bilgin*
Middle East Technical University, Ankara, Turkey
Murat Bronz†
ENAC, École Nationale de l'Aviation Civile, Université de Toulouse, Toulouse, France
Ilkay Yavrucuk‡
Technical University of Munich, Munich, Germany

ABSTRACT

In this study, previously proposed panel method based guidance algorithm is tested in a high fidelity simulation environment and in real-life scenarios with a fixed wing mini unmanned aerial vehicle. Panel method is a numerical tool, borrowed from fluid dynamics domain, that can generate collision free, smooth paths in environments with arbitrarily shaped obstacles. It guarantees convergence to global minima with little computational load. Local vector field generated by the panel method is used to demonstrate a simple path-planning and guidance of the fixed wing micro aerial vehicle with hardware experiments. Experimental results suggest that the proposed algorithm can generate collision free paths for a fixed wing aircraft without violating the vehicle's limited flight envelope.

http://www.imavs.org/

1 INTRODUCTION

In the air transportation industry, fuel cost and expenses associated with manpower are the first and second largest cost components respectively [1]. Therefore, having fully autonomous vehicles is desirable. Without a pilot present to operate the vehicles, path planning and guidance become important issues to be addressed.

The goal of path planning is to determine a collision-free path for a vehicle from an initial point to a target location. The path planning problem is usually mathematically large in size and computationally expensive, often hard to solve even offline. Therefore, methods that provide fast solutions to dynamic trajectory generation for aerial vehicles, while providing obstacle avoidance and collision avoidance are valuable [2].

Path planning for unmanned aerial vehicles (UAV) is well studied in literature. Classical approaches in path planning for autonomous vehicles in literature can be divided into two sub categories: optimization problem based methods and potential field based methods. The first approach is formulating the problem as a large optimization problem with constraints. Different cost functions can be considered to optimize time, distance, energy consumption, number of maneuvers, etc. Constraints may include dynamics of the vehicle and air traffic regulations[3, 4, 5, 6]. Second approach is employing potential functions where repulsive functions prevent collisions and attractive functions guide the vehicle to its destination [7]. Potential field method for path planning is applied in various fields from wheeled ground vehicles to unmanned aerial vehicles [8, 9, 10, 4, 11, 12]. Main advantage of this approach is its simplicity and easy implementation. The potential field method suffers from two major drawbacks. First one, the vehicle may get trapped in a local minima and secondly, the vehicle cannot reach to its destination if there are obstacles nearby due their repulsive force [13, 14]. Harmonic potential fields, a sub category of potential field based approaches, overcome the local minima limitation and produce constrained and well-behaved robot trajectory in static and dynamic environments [15, 16, 17, 18, 19]. An example of harmonic potential field is the potential field of an irrotational flow of an ideal fluid [20, 12]. The stream functions and streamlines can be obtained by using the potential field and then used as vehicle trajectories for solving the problem of navigation with obstacle avoidance. Analytical solutions can be obtained by combining elementary potentials such as uniform flow, sink, source and vortex, can only be used to generate collision free paths around relatively simple geometries, such as cylinders [21, 22]. To compute the velocity field around complex shaped obstacles a numerical tool, namely panel method can be employed. Previously, panel methods were used for robot motion planning and target tracking [23, 24, 25, 2].

More recently, panel method solution is used for addressing path planning problem in urban air mobility [26], where assuming complete knowledge of the city map, path of each vehicle in an air taxi fleet is determined simultaneously using panel method. Panel method based guidance algorithm was previously tested on quad-rotor platform [27, 28]. Quadrotors do not suffer from minimum speed of turn radius limitations. Hence, following the desired path is not a problem. On the other hand, fixed wing aircraft would stall at low speeds or cannot go backwards or sideways etc. There-

*Email address: e188254@metu.edu.tr
†Email address: murat.bronz@enac.fr
‡Email address: ilkay.yavrucuk@tum.de

http://www.imavs.org/

fore, generating paths that can be followed by a fixed-wing UAV is a challenging task.
In this paper the method proposed in [26] is tested for fixed-wing platform in a realistic simulation environment and hardware experiments are conducted in France. Experiments are held in a local RC airfield runway located in Muret, France. Aim of this study is to test the previously proposed panel method based guidance algorithm [27, 28] with a fixed wing aircraft.

2 GUIDANCE METHODOLOGY

This paper follows the panel method based guidance algorithm that was previously studied[26, 27, 28].

2.1 Panel Method Preliminaries

Panel method is a numerical tool commonly used in fluid mechanics and aerodynamics domain for calculating the velocity field of the irrotational flow of an ideal fluid around arbitrarily shaped objects. Panel method calculations require the surfaces of the obstacles to be divided into discrete elements called panels (hence the name panel method) as shown in Figure 1. Then, each panel is assigned a flow element (such as sources, doublets or vortices) with unknown strength. In this study, prescribed flow elements are selected as point vortices.

Let D be a region in $\Re^2$ containing an ideal fluid and

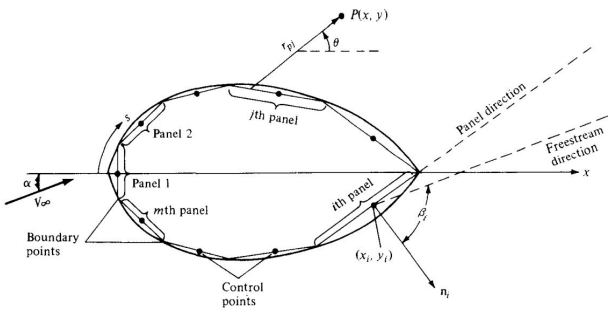

Figure 1: Panel distribution over the surface of a body of arbitrary shape [29].

$\boldsymbol{P} = (x, y)$ be any point in D. Velocity of the fluid can be described as $\boldsymbol{V} = (u, v)$. By Biot-Savart Law, velocity induced by a point vortex element placed at jth panel on any point $\boldsymbol{P} \in D$ can be calculated in terms of unknown vorticity strength γ as shown in Equations 1 and 2.

$$u = \frac{\gamma_j}{2\pi} \frac{(y_j - y)}{r_{pj}^2} \tag{1}$$

$$v = -\frac{\gamma_j}{2\pi} \frac{(x_j - x)}{r_{pj}^2} \tag{2}$$

where $(x_j, y_j)^T$ denotes the position of the point vortex and $r_{pj} = \sqrt{(x - x_j)^2 + (y - y_j)^2}$ is the distance between point vortex element and the point $\boldsymbol{P} = (x, y)^T$. Similarly, velocity induced by jth panel on ith panel can be expressed as $\boldsymbol{V}_{ij} = (u, v)_{ij}$ given in Equation 3.

$$\begin{bmatrix} u \\ v \end{bmatrix} = \frac{\gamma_j}{2\pi r_{ij}^2} \begin{bmatrix} 0 & 1 \\ -1 & 0 \end{bmatrix} \begin{bmatrix} x_j - x_i \\ y_j - y_i \end{bmatrix} \tag{3}$$

To find the unknown vorticity a boundary condition has to be enforced: the normal component of velocity induced at obstacle surface has to be zero such that no flow can go in or out of the obstacle boundary. After applying this boundary condition, panel method problem can be expressed as a system of linear equations given in Equation 4.

$$K_{ij}\gamma_j = RHS_i \tag{4}$$

$$K_{ij}\gamma_j = (u, v)_{ij} \cdot \vec{n_i} \tag{5}$$

Here, K is a coefficient matrix and γ_j is the unknown vortex strength on panel j. Components of K_{ij} are the normal velocity induced by jth panel on ith panel as given in Equation 5.

$$RHS_i = -u_\infty \cos\beta_i - v_\infty \sin\beta_i \tag{6}$$

The vector RHS consists of normal component of free stream velocity. Solution of the system of linear equations given in Equation 4 gives the unknown vortex strengths on obstacle surface.
When the strength of every flow element in the region $D \in \Re^2$ is known, the fluid velocity at any point can be calculated using Equations 1 and 2 .
Panel method is well studied in fluid mechanics and aerodynamics domain. Reader may refer to [29, 22] for detailed derivation of panel method.

2.2 Panel Method in Guidance Problem

After solving Equation 4 for unknown vortex strengths, fluid streamlines can be obtained. By definition fluid streamlines do not cross each other and avoid collision with objects on their path. Hence, resultant streamlines can be used as vehicle trajectories.
Following [26, 27, 28], panel method equations are further modified to fit the needs of the guidance problem.
First, a point sink element is introduced in RHS vector to represent a goal position for the vehicle (Equation 7).

$$\begin{aligned} RHS_i = &- u_\infty \cos\beta_i - v_\infty \sin\beta_i \\ &- u_{sink} \cos\beta_i - v_{sink} \sin\beta_i \end{aligned} \tag{7}$$

Panel method has built in obstacle avoidance property as streamlines cannot cross obstacle surfaces; however, to avoid collisions between vehicles and additional element is required. To that end, each vehicle is modeled as a point source element and the velocity induced by these sources are included in RHS vector as in Equation 8.

$$\begin{aligned} RHS_i = &- u_\infty \cos\beta_i - v_\infty \sin\beta_i \\ &- \sum_{n=1}^{N} u^n_{source} \cos\beta_i - \sum_{n=1}^{N} v^n_{source} \sin\beta_i \\ &- u_{sink} \cos\beta_i - v_{sink} \sin\beta_i \end{aligned} \tag{8}$$

Finally, to increase the safety perimeter around the obstacles *safety source element* introduced in [27] is included in RHS vector in Equation 9.Safety source element is an point source element that travels with the vehicle itself. The safety source element amplifies the vortex strengths on the obstacle edges that are in the vicinity of the vehicle. Consequently, obstacles push the vehicle further away to a safer distance.

$$\begin{aligned} RHS_i = &- u_\infty \cos\beta_i - v_\infty \sin\beta_i \\ &- \sum_{n=1}^{N} u^n_{source} \cos\beta_i - \sum_{n=1}^{N} v^n_{source} \sin\beta_i \\ &- u_{sink} \cos\beta_i - v_{sink} \sin\beta_i \\ &- u_{safety} \cos\beta_i - v_{safety} \sin\beta_i \end{aligned} \tag{9}$$

Here, u_∞ and v_∞ are components of free stream velocity. N is the total number of vehicles. u_{source} and v_{source} are velocities induced by point source elements. u_{sink} and v_{sink} velocity induced by sink element that represents the goal position. u_{safety} and v_{safety} are the velocities induced by *safety source element* introduced in [27].
After all the unknown vortex strengths are found, flow velocity $V = (u, v)$ at any point $P = (x, y) \in D$ can be calculated using the relation given in Equation 10 and Equation 11.

$$u = \frac{-\sigma}{2\pi}\frac{x - x_g}{r_g^2} + \sum_{n=1}^{N}\frac{\sigma_n}{2\pi}\frac{x - x_n}{r_n^2} + \sum_{s=1}^{S}\sum_{k=1}^{K}\frac{\gamma_{sk}}{2\pi}\frac{x - x_{sk}}{r_{sk}^2} \tag{10}$$

$$v = \frac{-\sigma}{2\pi}\frac{y - y_g}{r_g^2} + \sum_{n=1}^{N}\frac{\sigma_n}{2\pi}\frac{y - y_n}{r_n^2} + \sum_{s=1}^{S}\sum_{k=1}^{K}\frac{-\gamma_{sk}}{2\pi}\frac{y - y_{sk}}{r_{sk}^2} \tag{11}$$

Here, goal position is denoted by $P_g = (x_g, y_g)$ and sink strength associated with this goal position is σ. N is the total number of vehicles in the arena and each vehicle has a source assigned to them with strength σ_n. Position of vehicles are denoted as $P_n = (x_n, y_n)$. S and K are number of obstacles and number of panels respectively. Position of a vortex element on a given obstacle and panel is denoted as (x_{sk}, y_{sk}) and associated vortex strength is γ_{sk}. the Euclidean distance between the point P and the goal position is given as r_g. Similarly, r_n is the Euclidean distance between point P and nth vehicle in the region and r_{sk} is the distance between point P and kth panel on obstacle s.

2.3 *Panel Method and Automatic Flight Controller Integration for Guidance*

Block diagram for panel method based guidance is presented in Figure 2. Panel method requires vehicle positions

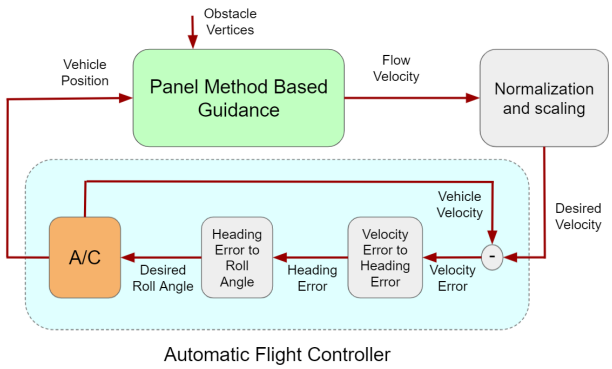

Figure 2: Block diagram for panel method based guidance.

and obstacle position as input. First, Equation 4 has to be solved for unknown vortex strengths. Coefficient matrix K in Equation 4 is a constant and can be calculated and inverted offline to reduce computational load. After vortex strengths are found, flow velocity at current vehicle position can be calculated using Equation 10 and Equation 11. This velocity has to be normalized and scaled. Flow velocity is greater in narrow passages and near goal position; however, the opposite velocity regime is safer and more desirable for vehicles. Hence, flow velocity is also inverted before being fed into automatic flight control system as desired velocity.
Automatic flight controller calculates velocity error and converts it to heading error following the method presented in [30]. Then, heading error is converted to roll angle error constraint by a sustained turn. Finally, desired roll angle is fed to the vehicle.

Reader may refer to [26, 27, 28] for detailed derivation of method.

3 EXAMPLE SCENARIO

In this study, panel method based guidance algorithm is utilized for a fixed wing aircraft flying in an outdoor arena with several no-fly zones. Figure 3 shows an example flight arena. Here horizontal axis is East direction and vertical axis is North direction. All distance units are in meters. Solid magenta shapes represent the no-fly zones and act as obstacles in panel method calculations. One of the strengths of panel method is that it can generate a flow field around arbitrarily shaped objects. Lighter colored regions around no-fly zones are the safety perimeters that are obtained by inflating the object boundaries by an amount of $5m$.

In Figure 4, streamlines and paths followed by different vehicles are plotted. Start position is indicated with a blue circle and goal position is marked with x. At the start position, using the formula given in Equations 10 and 11, desired

http://www.imavs.org/

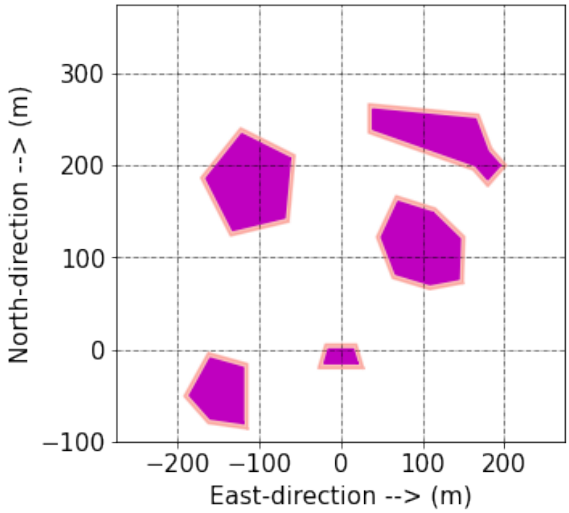

Figure 3: Example flight arena.

velocity is calculated. This desired velocity is normalized and fed to the vehicle as a desired heading command. As the vehicle travels in the desired direction, flow velocity calculation is repeated for new position and desired heading command is updated until the vehicle reaches its goal position. Paths plotted in Figure 4a and Figure 4b are the resultant trajectories followed by vehicles from indicated start position to marked goal position. In both cases, vehicles converge to goal position following the streamlines. Since all streamlines lead to the sink placed at the goal position, vehicles would arrive to the destination irrespective of their start position. Furthermore, since goal position can be placed any point on the map, collision free path between any point on the map can be generated.

4 IMPLEMENTATION AND FLIGHT PERFORMANCE

For simulations and real-flight experiments, open-sourced Paparazzi Autopilot system [31] has been employed. The simulation environment resorts on the JSBSIM flight dynamics model and presents a sufficiently realistic demonstration during the development of the panel-method based guidance algorithm. In the following sections, detailed description of the test platform and the flight experiments are discussed.

4.1 Experimental Platform

An overview of the complete flight test system is shown in Figure 5a. A small fixed-wing UAV has been used for the real-flight experiments. A laptop running Unix/Linux for Ground Control Station is used to control the autonomous mission and also to send the reference velocity input calculated by the panel-method based guidance algorithm during flight. An X-Bee radio modem, attached on the side of the computer screen in Figure 5a, is utilized for telemetry between the aircraft and the Ground Control Station and datalink communication was sufficient as the flight tests were

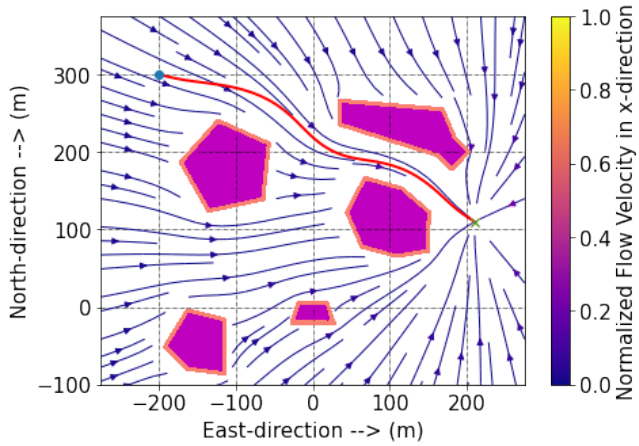

(a) Streamlines and path of vehicle 1.

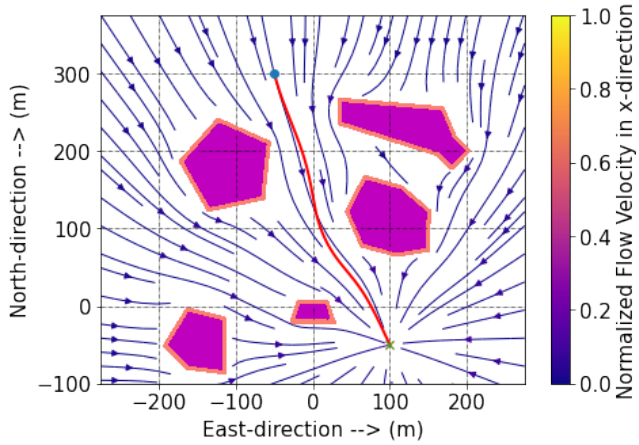

(b) Streamlines and path of vehicle 2.

Figure 4: Streamlines and paths of vehicles with different start positions and destinations.

done within 500 m radius. An RC-Transmitter is used to ensure the safely recovering of the vehicle in case of loss of control in autonomous mode or any unprecedented situation.

4.2 Flight Experiments

Outdoor runway experiments are conducted in a local RC airfield runway located in Muret, France, that is 124 m $\times$ 12.5 m in size, as shown in Fig. 5b.

ENAC has privileged access to this airfield, and can do tests in a volume of 500 m radius and up to 150 m height (which can be increased to 450 m in certain cases).

For outdoor flight experiments, 2 scenarios are considered. The mission for the first scenario is plotted in Figure 6. Before the mission starts, aircraft is loitering around a standby position just outside the flight mission arena indicated with a start arrow on Figure 6a. Standby position is marked with a red diamond in lower right corner of Figure 6b, and

http://www.imavs.org/

(a) Complete flight test system that is used during the flights.

(b) Outdoor flight facility at Muret, France.

Figure 5: Complete flight test system and flight facility.

Specification		Units
Wing Span	1.2	[m]
Surface Area	0.28	[m^2]
Mass	0.75	[kg]
Battery Capacity	30	[Wh]
Flight speed	12	[m/s]
Flight time	60	[min]
Components		
Motor	T-Motor 2208/18 - Kv 1100	
Autopilot	Paparazzi Chimera v1.0 [1]	
GPS	U-Blox M8N	
Companion board	Raspberry Pi Zero v 1.3	

Table 1: Airframe Specifications

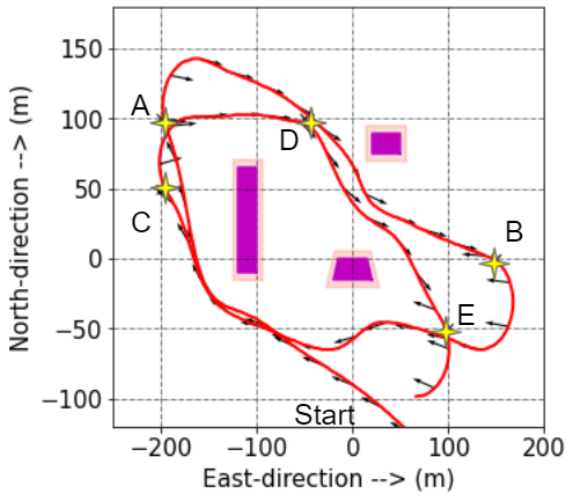

(a) Simulated path and desired velocity vectors.

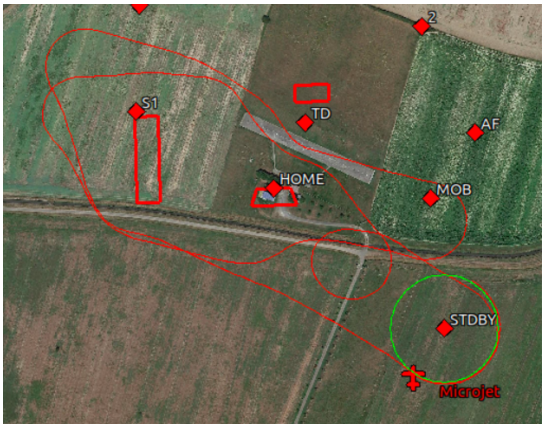

(b) Simulation for flight facility at Muret, France.

Figure 6: Simulations for Scenario 1.

loiter path is indicated with a green circle around standby point. Goal positions are marked with stars in Figure 6a and no-fly zones are painted with magenta. Furthermore, no-fly zones can also be observed in Figure 6b as red polygons. The mission of the aircraft for the first scenario is to travel between points A-B-C-D-E sequentially without entering the no-fly zones. After reaching point E the vehicle repeats the sequence until it is called back to standby position again. Arrows plotted on the path in Figure 6a are the instantaneous flow velocity calculated by panel method. The difference between the instantaneous flow velocity plotted here and the vehicle velocity is used for heading error calculation in automatic flight controller as discussed in Section 2. For all simulated cases, ground speed of the vehicle was at $13m/s$ and maximum bank angle was limited to 30 degrees.

In Figure 7, path logged in real flight test for scenario 1 in Muret, France is plotted. In this case, the vehicle is to travel between points A-B-C-D-E and repeat the task until it is called back to standby position. Although path followed by the vehicle in real flight is slightly different from the simulated case, the vehicle successfully completes the mission several times without entering into the no-fly zones.

Since all the equations in panel method is non-dimensional, it can be scaled to larger problems. In that respect the second

http://www.imavs.org/

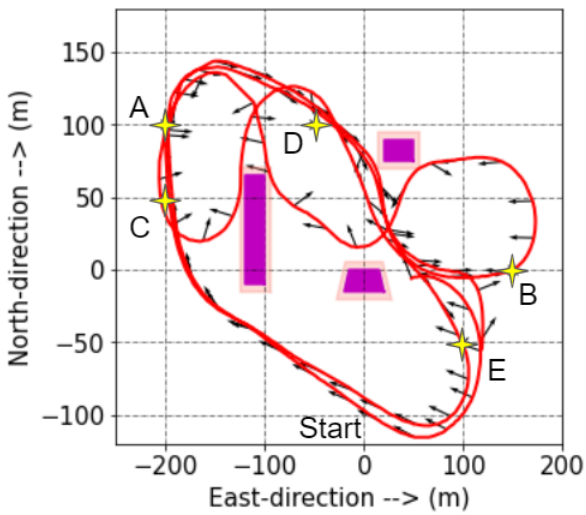

Figure 7: Real flight log for Scenario 1.

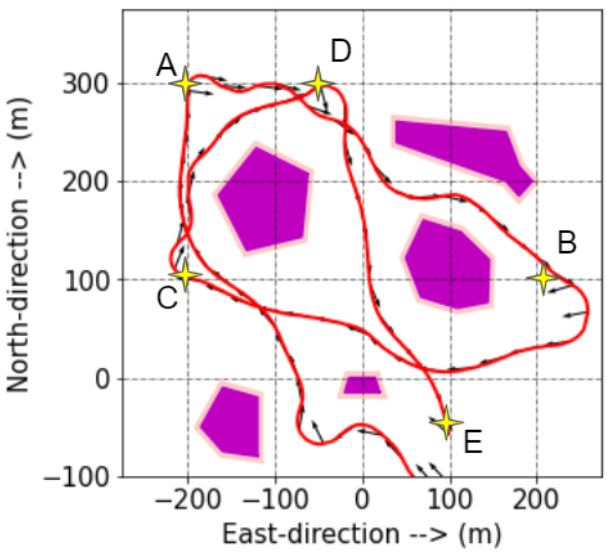

Figure 8: Real flight log for Scenario 2.

scenario is conducted in a larger airspace as shown in Figure 8. Moreover, instead of rectangles, this second arena also contains arbitrarily shaped no-fly zones. Again, the vehicle is loitering around the stand by position outside the map. The mission is to travel between point A-B-C-D-E sequentially and returning to point A again to repeat the task.
In scenario 1, relatively smaller arena is used. When confined in a such narrow space, minimum turn radius of the fixed wing aircraft becomes a limiting factor. Conversely, in scenario 2 much larger area is used; thus, there was enough space for maneuvers at goal locations. To make this scenario more interesting no-fly zones placed to create narrow corridors between goal locations. For real flights, the ground speed of the vehicle was set to $15m/s$ and maximum bank angle was limited to 50 degrees.

5 CONCLUSION AND FUTURE WORK

This study focuses on experimental evaluation of the method presented in [27, 28] on fixed wing platform. Guidance for a fixed wing aircraft is a challenging task due to the constraints on minimum speed and turn radius. Panel method imitates fluid flow and generates easy to follow smooth trajectories for vehicles. Simulations and flight experiments indicate that fixed wing aircraft can follow the collision free paths generated by panel method without exceeding the flight envelope limits.
As future work, panel method algorithm can be further improved to generate even smoother paths that can guarantee both obstacle avoidance and envelope protection.

ACKNOWLEDGEMENTS

The authors would like to thank to Xavier Paris for his support during outdoor flight tests. The author Z. Bilgin was funded by Campus France.

REFERENCES

[1] M. Ball, C. Barnhart, G. Nemhause, and A. Odoni. Air transportation: irregular operations and control. *Handbooks Oper. Res. Manage. Sci.*, 14:1–67, 2007.

[2] Oguz Uzol, Ilkay Yavrucuk, and Nilay Sezer Uzol. Panel-method-based path planning and collaborative target tracking for swarming micro air vehicles. *Journal of Aircraft*, 47(2).

[3] M.Mirzaei Teshnizi, A. Kosari, S. Goliaei, and S. Shakhesi. Centralized path planning for multi-aircraft in the presence of static and moving obstacles. *International Journal of Engineering*, 33(5).

[4] Yongbo Chen, Guanchen Luo, Yuesong Mei, Jianqiao Yu, and Xiaolong Su. Uav path planning using artificial potential field method updated by optimal control theory. *International Journal of Systems Science*, 2014.

[5] Dantong Ge and Ufuk Topcu. Hierarchical path planning for urban on-demand air mobility. In *2019 IEEE Conference on Control Technology and Applications (CCTA)*, August 19-21 2019.

[6] Priyank Pradeep and Peng Wei. Energy-efficient arrival with rta constraint for multirotor evtol in urban air mobility. *Journal of Aerospace Information Systems*, 16(7).

[7] O. Khatib. Real-time obstacle avoidance for manipulators and mobile robots. In *Proceedings. 1985 IEEE International Conference on Robotics and Automation*, volume 2, pages 500–505, 1985.

[8] Ulises Orozco-Rosas, Oscar Montiel, and Roberto Sepúlveda. Mobile robot path planning using membrane

http://www.imavs.org/

evolutionary artificial potential field. *Applied Soft Computing Journal*, pages 236–251, April 2019.

[9] Liu Lifen, Shi Ruoxin, Li Shuandao, and Wu Jiang. Path planning for uavs based on improved artificial potential field method through changing the repulsive potential function. In *Proceedings of 2016 IEEE Chinese Guidance, Navigation and Control Conference*, August 12-14 2016.

[10] Z. Yingkun. Flight path planning of agriculture uav based on improved artificial potential field method. In *2018 Chinese Control And Decision Conference (CCDC)*, 2018.

[11] Yuecheng Liu and Yongjia Zhao. A virtual-waypoint based artificial potential field method for uav path planning. In *Proceedings of 2016 IEEE Chinese Guidance, Navigation and Control Conference*, August 12-14 2016.

[12] H. Wang, W. Lyu, P. Yao, X. Liang, and C. Liu. Three-dimensional path planning for unmanned aerial vehicle based on interfered fluid dynamical system. *Chinese Journal of Aeronautics*, 28(1).

[13] Weihao Li, Chenguang Yang, Yiming Jiang, Xiaofeng Liu, and Chun-Yi Su. Motion planning for omnidirectional wheeled mobile robot by potential field method. *Journal of Advanced Transportation*, 2017:1–11, 03 2017.

[14] Seyyed Mohammad Hosseini Rostami, Arun Kumar, Jin Wang, and Xiaozhu Liu. Obstacle avoidance of mobile robots using modified artificial potential field algorithm. *EURASIP Journal on Wireless Communications and Networking*, 2019, 03 2019.

[15] J.-O. Kim and P.K. Khosla. Real-time obstacle avoidance using harmonic potential functions. *IEEE Transactions on Robotics and Automation*, 8(3):338–349, 1992.

[16] Ahmad A. Masoud. A harmonic potential field approach for joint planning and control of a rigid, separable nonholonomic, mobile robot. *Robotics and Autonomous Systems*, 61(6):593–615, 2013.

[17] Farbod Fahimi. *Autonomous robots*. Springer, 2010.

[18] Robert Daily and David M. Bevly. Harmonic potential field path planning for high speed vehicles. In *2008 American Control Conference*, pages 4609–4614, 2008.

[19] Santiago Garrido and Luis Moreno. Robotic navigation using harmonic functions and finite elements. pages 94–103, 01 2006.

[20] X. Liang, H. Wang, D. Li, and C. Liu. Three-dimensional path planning for unmanned aerial vehicles based on fluid flow. In *2014 IEEE Aerospace Conference*, 2014.

[21] R. I. Lewis. *Vortex Element Methods for Fluid Dynamic Analysis of Engineering Systems*. Cambridge Univ. Press, Cambridge, UK, 1991.

[22] J. Katz and A. Plotkin. *Low Speed Aerodynamics*. Cambridge Univ. Press, Cambridge, UK, 2001.

[23] Y. Zhang and K. P. Valavanis. A 3-d potential panel method for robot motion planning. *Robotica*, 15(4).

[24] Jasmin Velagic, Lamija Vuković, and Belma Ibrahimovic. Mobile robot motion framework based on enhanced robust panel method. *International Journal of Control, Automation and Systems*, 18, 11 2019.

[25] Jasmin Velagić, Lamija Vuković, and Belma Ibrahimović. Mobile robot motion framework based on enhanced robust panel method. *International Journal of Control, Automation and Systems*, 18(5):1264–1276, 2020.

[26] Zeynep Unal and Ilkay Yavrucuk. Panel method based path planning for evtol in urban environment. In *Vertical Flight Society Forum 77*, May 10-14 2021.

[27] Zeynep Bilgin, Murat Bronz, and Ilkay Yavrucuk. Experimental evaluation of panel-method-based path planning for evtol in a scaled urban environment. In *Vertical Flight Society Forum 78*, May 10-12 2022.

[28] Zeynep Bilgin, Murat Bronz, and Ilkay Yavrucuk. Experimental evaluation of robustness of panel-method-based path planning for urban air mobility. In *AIAA Aviation Forum*, 27 June-1 July 2022.

[29] John D. Anderson. *Fundamentals of Aerodynamics*. McGraw-Hill, 5th edition, 2011.

[30] Hector Garcia De Marina, Yuri A Kapitanyuk, Murat Bronz, Gautier Hattenberger, and Ming Cao. Guidance algorithm for smooth trajectory tracking of a fixed wing uav flying in wind flows. In *2017 IEEE international conference on robotics and automation (ICRA)*, pages 5740–5745. IEEE, 2017.

[31] Gautier Hattenberger, Murat Bronz, and Michel Gorraz. Using the Paparazzi UAV System for Scientific Research. In *International Micro Air Vehicles Conference and Flight Competition*, pages 247–252, Delft, Netherlands, 2014.

http://www.imavs.org/